Supplementary Materials

Flexible PTh/GQDs/TiO_2 Composite with Superior Visible-Light Photocatalytic Properties for Rapid Degradation Pollutants

Tong Li[a,†], Ru Li[a,†,], Lei Yang[b], Rong-Xu Wang[a], Rui Liu[a], Ye-Lin Chen[a], Shi-Ying Yan[a,*], Seeram Ramakrishna[c], and Yun-Ze Long[a,d,*]*

[a] Collaborative Innovation Center for Nanomaterials & Devices, College of Physics, Qingdao University, Qingdao 266071, China

[b] Research Center for Intelligent & Wearable Technology, College of Textiles & Clothing, Qingdao University, Qingdao 2266071, China

[c] Center for Nanofibers & Nanotechnology, Faculty of Engineering, National University of Singapore, Singapore

[d] State Key Laboratory of Bio-Fibers & Eco-Textiles (Qingdao University), Qingdao 266071, China

†These two authors contributed equally to this work.

*Corresponding author. Tel: +86 13953290681; E-mail addresses: liruouc@163.com (R. Li), ysy5954418@163.com (S.Y. Yan) and yunze.long@qdu.edu.cn (Y.Z. Long)

Table of Contents

1. Experimental Section

1.1 Materials

Polyvinylidene fluoride (PVDF, Mw & 550000) was obtained from Sigma-Aldrich (St. Louis, MO). N-dimethylformamide (DMF), Tetrabutyl Titanate (TBOT), Acetone, Ammonium persulfate [$(NH_4)_2S_2O_8$], Ferric chloride ($FeCl_3$), methylene blue (MB), methyl orange (MO), Hydrochloric acid (HCl), nitric acid (HNO_3), sodium hydroxide (NaOH), Silver nitrate ($AgNO_3$), ammonium oxalate (AO), p-benzoquinone (BQ) and isopropanol (IPA) were purchased from Sinopharm Chemical Reagents Co, LTD. Thiophene monomer, pyrrole monomer, TC and pyrene are provided by Shanghai Maclin Biochemical Co, LTD. Aniline and chloroform were purchased from Shanghai Aladdin Biochemical Technology Co, LTD. These chemicals were used in all experiments with analytic-grade, deionized and highly purified water.

1.2 Characterization

X-ray diffraction (XRD) data were obtained on a Rigaku Smart Lab X-ray diffractometer with Cu Kα radiation (0.1542 nm) using a step size of 0.02°. We observed the morphology of the samples using transmission electron microscopy (TEM, JEM-2100F) equipped with an energy-dispersive X-ray spectrometer (EDS, INCAx-Sight6427). Flourier transformed infrared spectroscopic (FTIR) spectra were obtained on a Nicolet iS50 spectrometer. The photoluminescence (PL) spectrum of the sample at the excitation wavelength of 320 nm was measured by the Hitachi F-4600 fluorescence spectrometer to study the recombination efficiency of a photoinduced charge. UV-visible diffuse reflection spectra (UV–Vis DRS) were recorded on a SOLID 3700 spectrophotometer. We utilized X-ray photoelectron spectroscopy (XPS, Thermo ESCALAB 250) signals to evaluate the samples' elements with an Al Ka X-ray source ($h\nu$ = 1486.6 eV) and pass energy of 30 eV. Photoelectrochemical measurement was performed by electrochemical workstation (CH Instruments CHI 660E scanning potentiostat). Three electrodes with sample, Pt electrode, and saturated calomel electrode were placed in the electrolyte of 0.5 $mol \cdot L^{-1}$ Na_2SO_4 aqueous solution.

The hybrid fiber membranes were cut into units of 1 cm × 1 cm and fixed on an indium tin oxide glass by conductive adhesive. Photocurrent density data were recorded every 20 s under an Xe lamp (300 W) with a UV cut filter (λ > 420 nm). The total organic carbon (TOC) assays were conducted on a Shimadzu TOC-L analyzer. The degradation intermediates of TC were identified by Ultimate 3000 UHPLC-Q precision liquid chromatography-mass spectrometry (LC-MS).

1.3 Preparation of graphene quantum dots

Graphene quantum dots (GQDs) is prepared in alkaline aqueous solution, where the presence of alkaline species enables the elimination of hydrogen, condensation or graphitization and edge functionalization. Before the alkaline hydrothermal treatment, pyrene was required to be nitrated into 1,3,6-trinitropyrene in hot HNO_3. GQDs were typically synthesized by the nitration of pyrene in hot nitric acid at 80 °C followed by hydrothermal treatment in 0.2 $mol \cdot L^{-1}$ NaOH aqueous solution at 200 °C for 10 h. After cooling to room temperature, the insoluble carbon products were removed by filtration to obtain water-soluble GQDs. The resulting solution is brown-black under natural light and green under ultraviolet light, which is fluorescent

1.4 Preparation of flexible PPy/GQDs/TiO_2 fiber membranes

PPy was in situ polymerized on GT film with methyl orange (MO) as soft membrane plate. Dissolve 1 $Mmol \cdot L^{-1}$ MO in 20 mL water, soak GT film in MO solution for 30 min, slowly drop into 1 $mol \cdot L^{-1}$ $FeCl_3$ solution for 30 min. After the mixture was cooled in an ice bath, 1 $mol \cdot L^{-1}$ pyrrole solution was dropped and polymerized at 2 °C for 2 h. The polymerized PPy/GT composite film was washed several times with distilled water and dried overnight at 70 °C in a vacuum oven. Molar mass ratio Ti: pyrrole monomer = 1:2.

1.5 Preparation of flexible PAn/GQDs/TiO_2 fiber membranes

PAn/GT fiber membrane is usually prepared by the method of 0.2 mL of aniline was added in 25 mL of 1 $mol \cdot L^{-1}$ HCI to get solution A, 0.08 g of ammonium persulfate was added to 25 mL of 1 $mol \cdot L^{-1}$ HCI to get solution B. The GT fiber membranes were soaked in solution A for 30 min,

subsequently, the solution B was added slowly and kept for 2 h to produce PAn/GT hybrid membranes. The membranes were washed with deionized water for several times before dried at 50 °C in vacuum oven overnight. Molar mass ratio Ti: aniline monomer = 1:2.

2. Figures and Tables

Detail information of CPs/GT flexible fiber membranes:

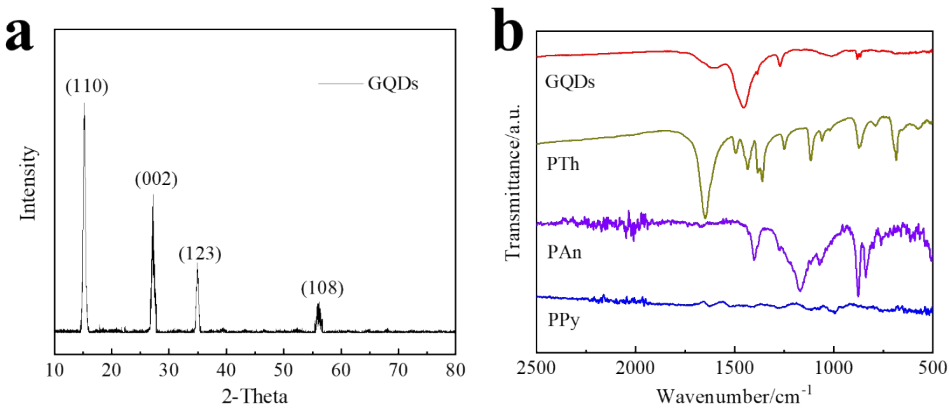

Fig. S1 (a) XRD patterns of GQDs and (b) the FTIR diagrams of pure polymers and GQDs.

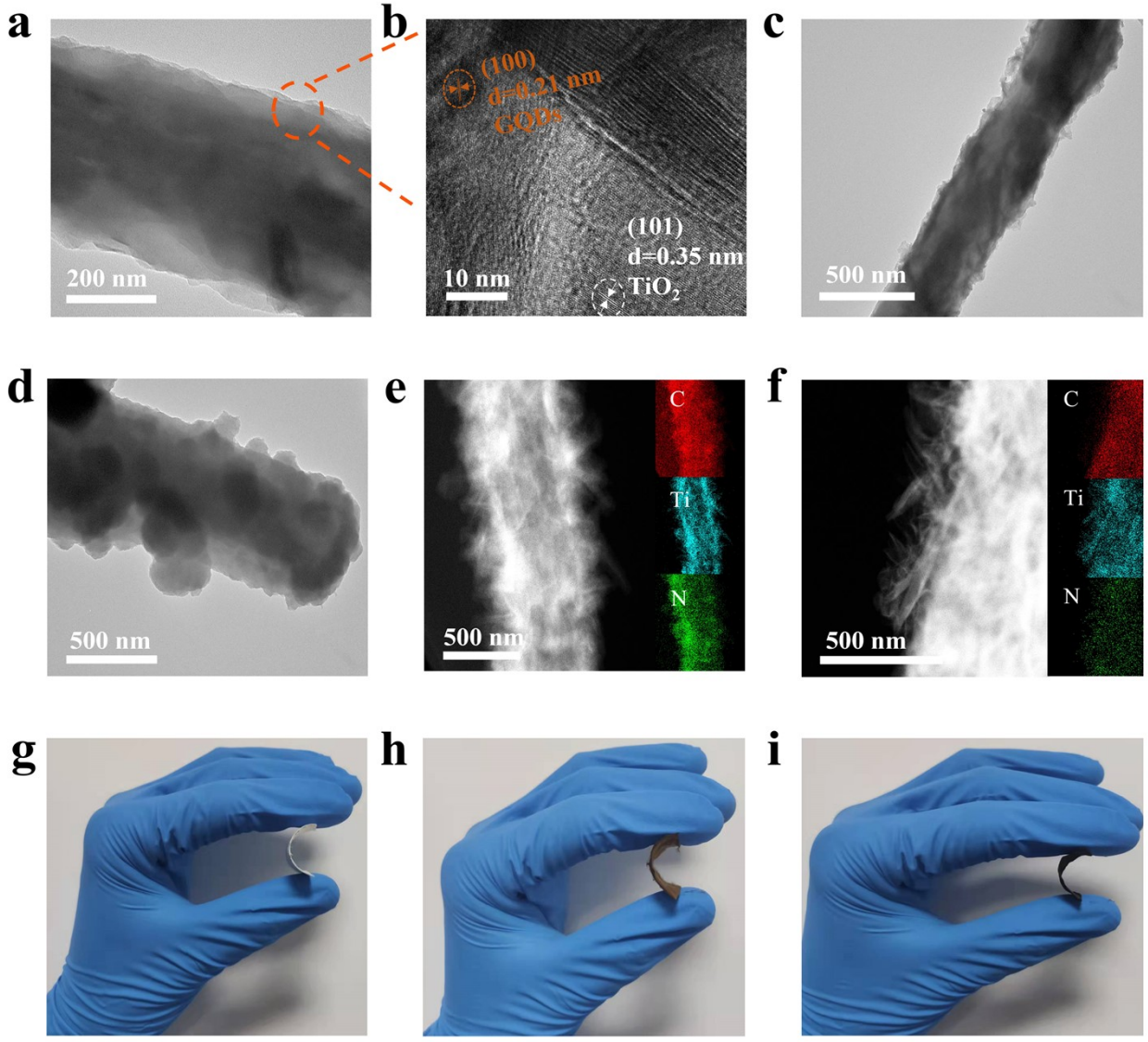

Fig. S2 (a, b) SAED pattern of GT. (c, d) TEM images of PPy/GT and PAn/GT fibers. (e, f) TEM image of PPy/GT and PAn/GT fibers with elemental mapping images of C, Ti and N, respectively, on an individual fiber. (g–i) Photographs showing the flexibility of the pure TiO_2, GT, and PTh/GT membrane.

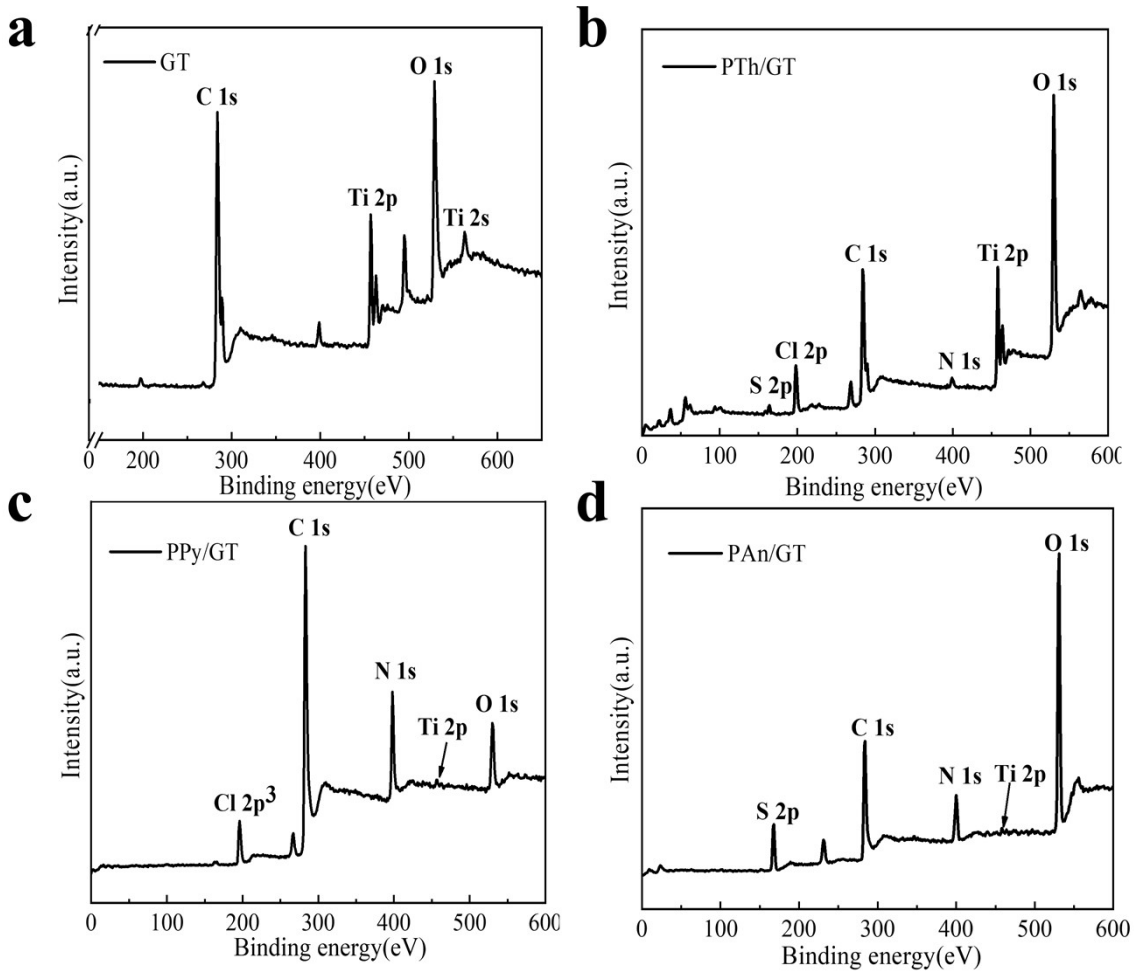

Fig. S3 Survey XPS spectrum of (a) GT, (b) PTh/GT, (c) PPy/GT and (d) PAn/GT fiber membranes.

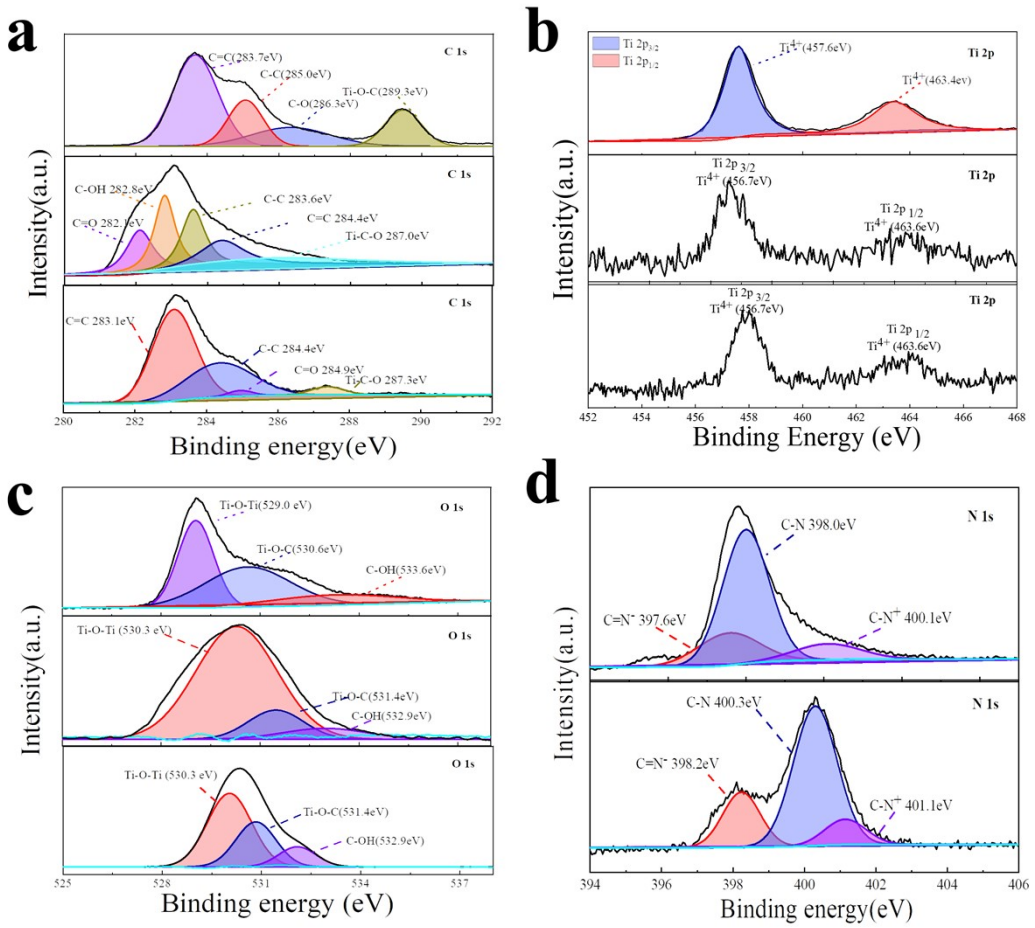

Fig. S4 The XPS peak data of GT, PPy/GT and PAn/GT fiber membranes are shown from top to bottom: (a) C 1s, (b) Ti 2p, (c) O 1s, (d) N 1s.

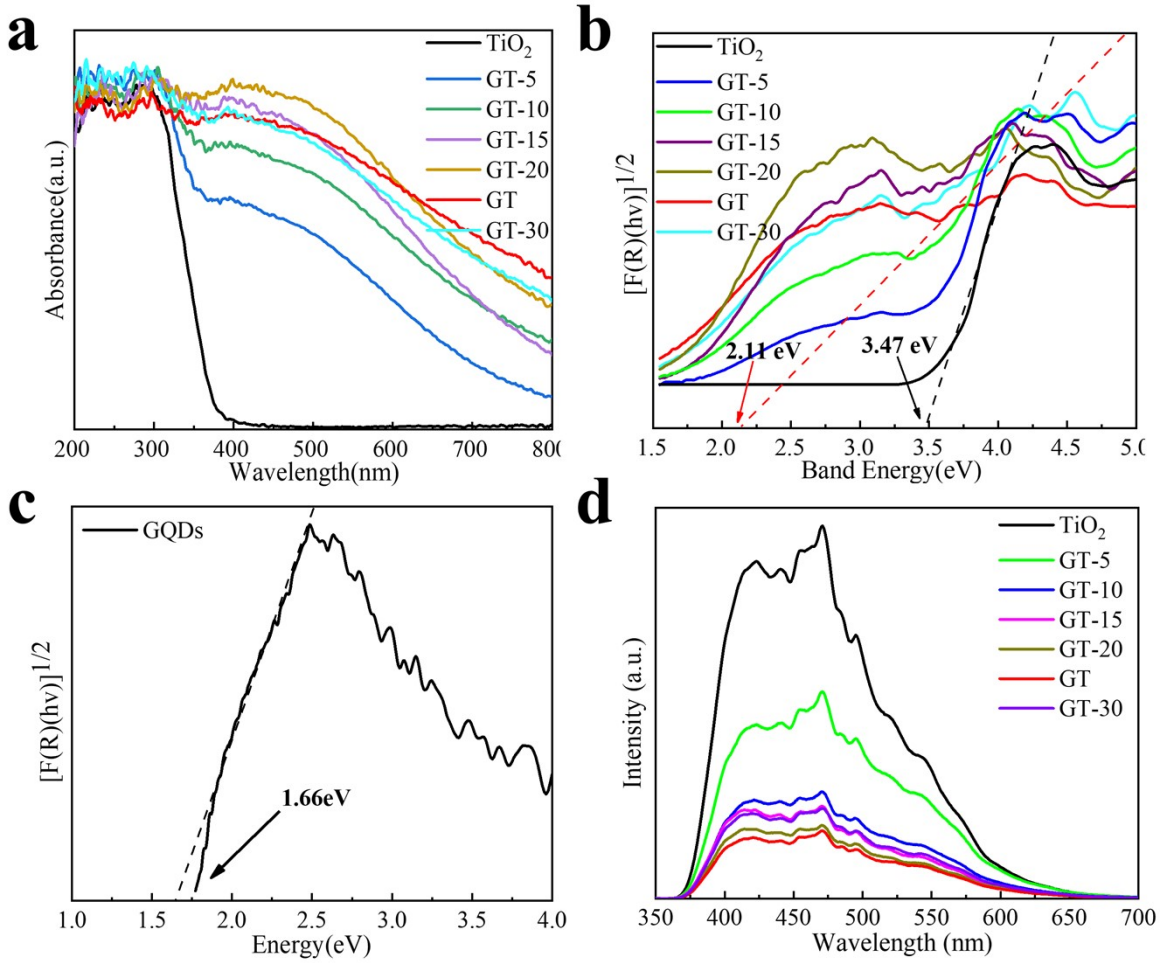

Fig. S5 Band structures of the as-prepared different ratio of GQDs and TiO_2 fiber membranes. (a) UV-Vis diffuse reflection spectra, (b) plot of $[F(R)h\nu]^{1/2}$ *vs*. photon energy of different samples and (c) pure GQDs, (d) PL spectra.

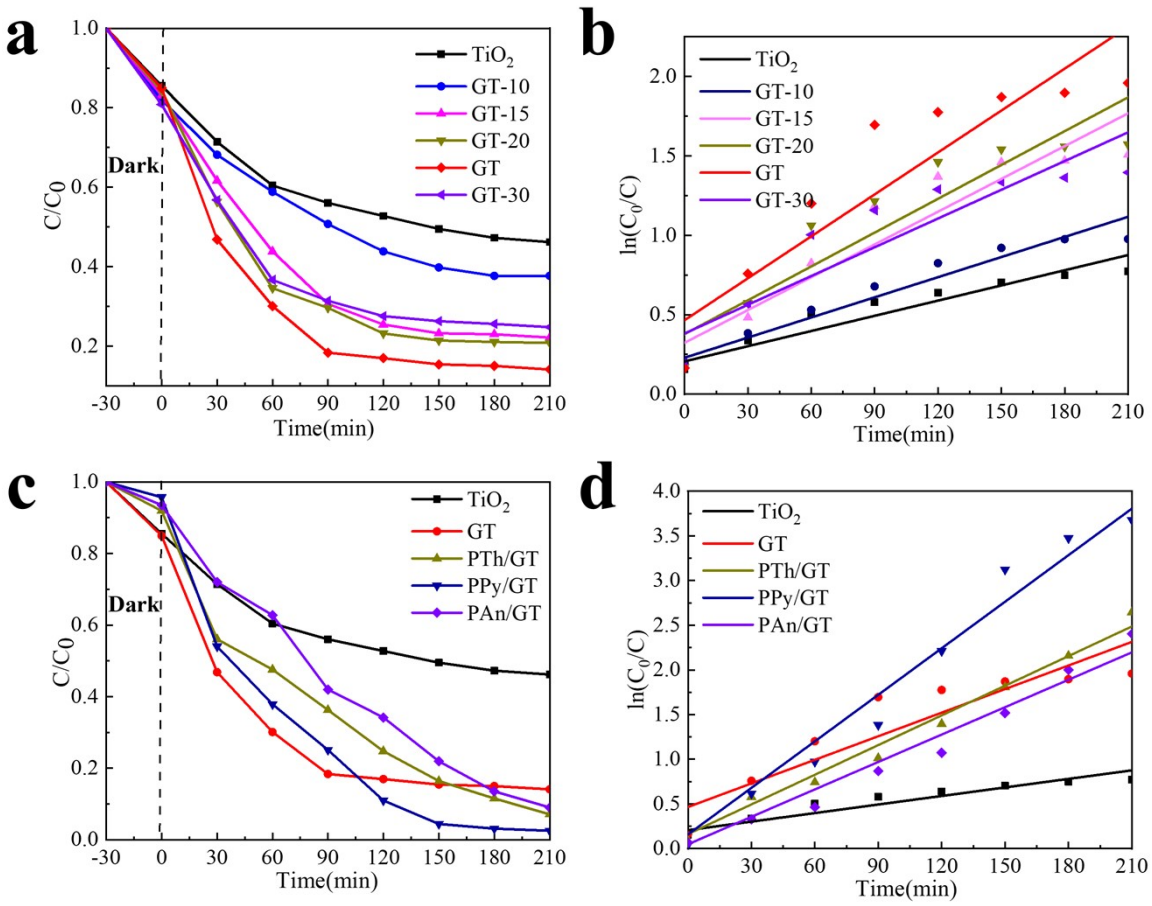

Fig. S6 Photocatalytic degradation of MB for different catalyst samples. (a, c) Photocatalytic degradation efficiency of MB solution by different samples and (b, d) Plot of ln(C_0/C) *vs*. irradiation time (t) for MB degradation in different catalysts.

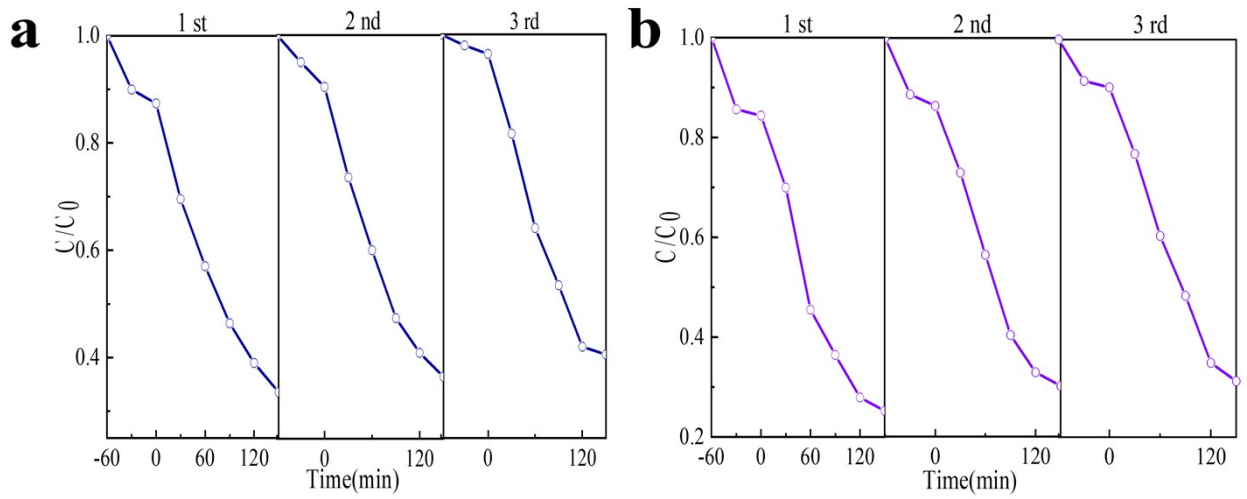

Fig. S7 Change in relative concentration of TC as a function of irradiation time for (a) PPy /GT and (b) PAn/GT catalyst for three repeated cycles, respectively.

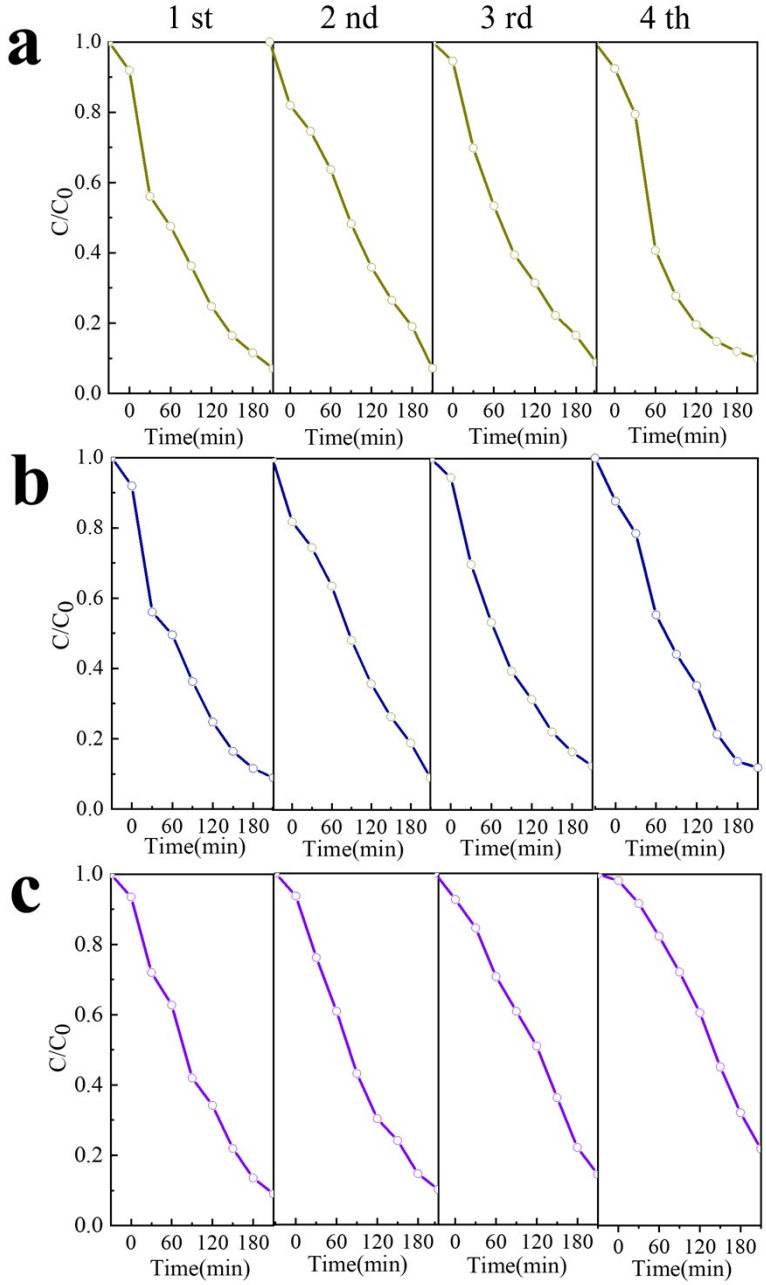

Fig. S8 Change in relative concentration of MB as a function of irradiation time for (a) PTh/GT, (b) PPy/GT and (c) PAn/GT catalyst for four repeated cycles.

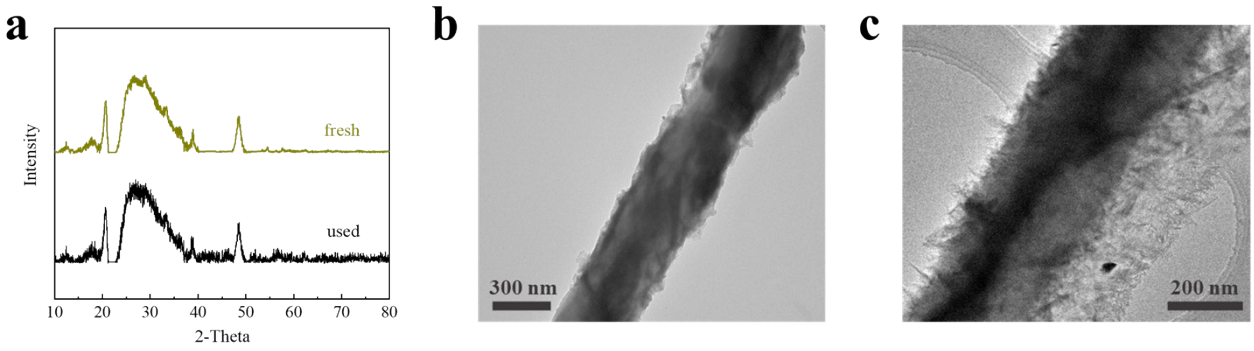

Fig. S9 Comparison of XRD (a) and SEM (b-c) before and after PTh/GT reuse.

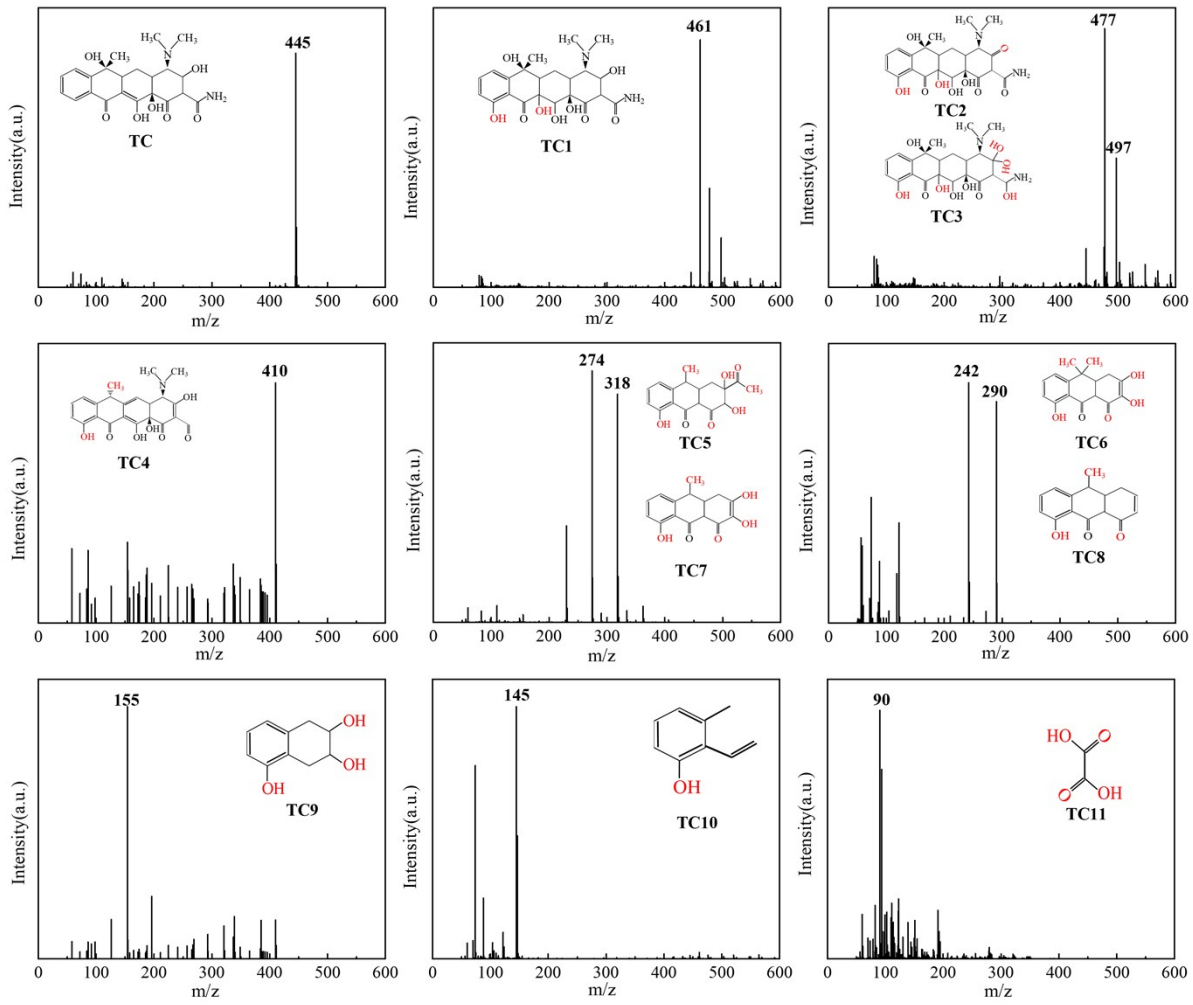

Fig. S10 LC-MS analysis results of visible-light photocatalytic degradation of TC over the PTh/GT. Catalyst amount 2 cm×2 cm, C_0=20 mg/L, light irradiation time 90 min and 210 min spectra of the TC and possible intermediates.

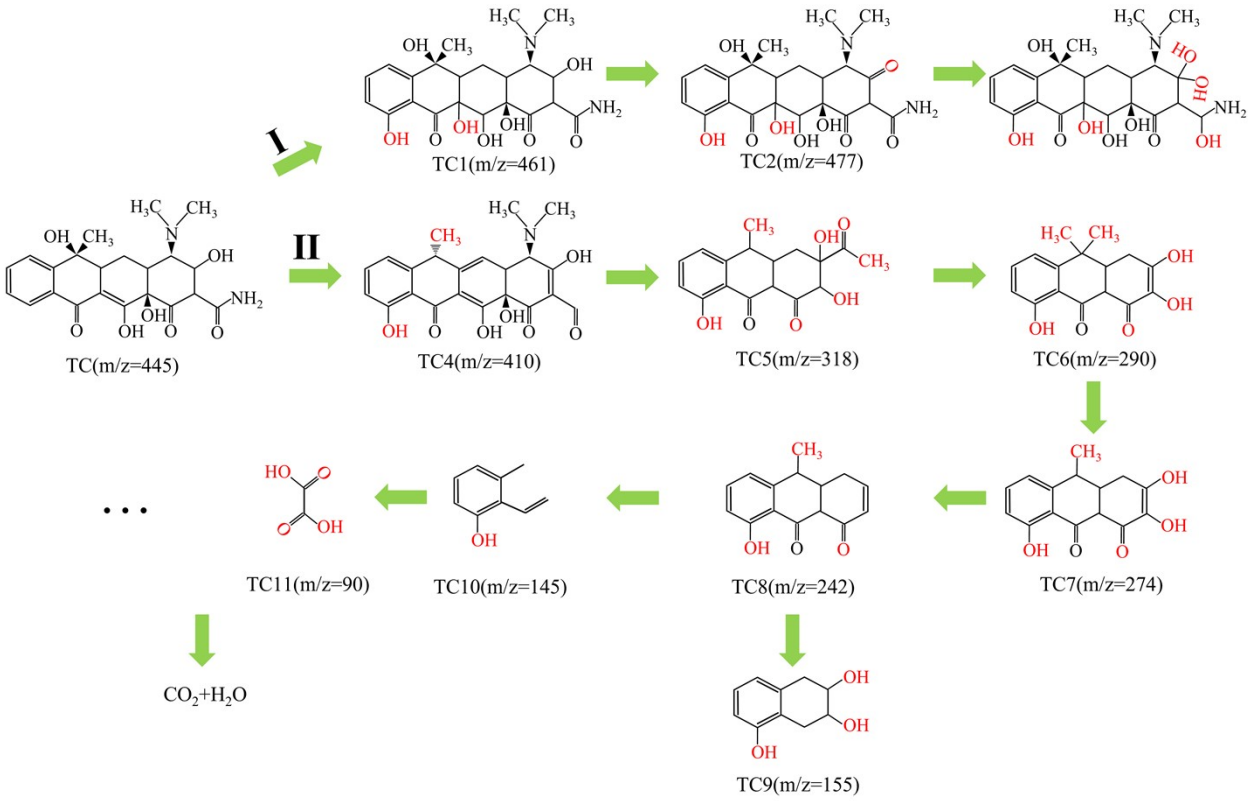

Fig. S11 Two possible degradation pathways of TC were proposed in the PTh/GT system.

Table S1 The elemental composition of three CPs/GT derived from XPS.

sample	Element (Atomic %)	Element (Atomic %)	Element (Atomic %)	Element (Atomic %)	Element (Atomic %)
PTh/GT	C (41.32)	O (25.28)	Ti (5.41)	N (2.31)	S (1.87)
PPy/GT	C (69.33)	O (7.91)	Ti (0.37)	N (15.79)	
PAn/GT	C (44.62)	O (36.09)	Ti (0.26)	N (11.29)	

Table S2 Adsorption kinetic parameters of composite fiber membrane.

Sample	Pseudo-first-order			Pseudo-second-order			Intra-particle diffusion		
	q_e(mg g^{-1})	k_1(min^{-1})	R^2	q_e(mg g^{-1})	k_1(min^{-1})	R^2	c(mg g^{-1})	k_1(min^{-1})	R^2
TiO_2	2.36951	0.067	0.9475	2.36951	0.408	0.9997	2.3776	0.0641	0.9781
GT	1.99904	0.045	0.9201	1.99904	0.473	0.9962	2.0049	0.0729	0.9934
PTh/GT	1.48735	0.078	0.7751	1.48735	0.647	0.9987	1.4859	0.0352	0.9549
PPy/GT	2.45583	0.121	0.5906	2.45583	0.309	0.9904	2.4583	0.2865	0.9374
PAn/GT	2.45402	0.056	0.7145	2.45402	0.382	0.9956	2.4429	0.1329	0.7477

Table S3 The equilibrium adsorption parameters fitted by Langmuir and Freundlich models for TC adsorption.

Sample	Langmuir adsorption model			Freundlich adsorption model		
	q_{max}(mg g^{-1})	K_L (L mg^{-1})	R^2	n	K_F (mg·g^{-1})	R^2
TiO_2	2.3786	0.8091	0.9997	11.7941	1.8168	0.9926
GT	2.1524	0.3230	0.9960	6.7541	1.1885	0.9747
PTh/GT	1.5488	0.5333	0.9986	12.3235	1.1015	0.8963
PPy/GT	5.7192	0.0328	0.8536	1.3639	0.2510	0.8436
PAn/GT	2.7012	0.3605	0.9931	5.0357	1.3256	0.7252

Table S4 Comparison of removal ratio of TC for different photocatalyst.

Catalysts	Photocatalyst dosage	Initial concentration of TC (mg L^{-1})	Degradation rate (%)	Cycling stability times	Cycling stability decrease in efficiency (%)	Ref.
PTh/GQDs/TiO_2	**2 cm×2 cm**	**20**	**80.6**	**3**	**4**	**This study**
C/TiO_2	/	50	60.0	/	/	1
Black TiO_2	0.2 g·L^{-1}	10	66.2	4	3	2
N-TiO_2	0.2 g·L^{-1}	10	62.5	4	4.5	3
C-N-S- TiO_2	0.5 g·L^{-1}	25	71.0	/	/	4
In_2S_3/TiO_2	0.2 g·L^{-1}	40	78.1	/	/	5
MoS_2@MIL-53(Fe)	0.1 g·L^{-1}	20	42	/	/	6
BiOI	1 g·L^{-1}	20	69.4	4	20.4	7

References

1 W. Zhang, M. Gao, F. Miao, X. Wu, S. Wang, X. Wang, A permeable electrochemical reactive barrier for underground water remediation using TiO_2/graphite composites as heterogeneous electrocatalysts without releasing of chemical substances, *J. Hazard. Mater.*, 2021, **418**, 126318.

2 S. Wu, X. Li, Y. Tian, Y. Lin, Y.H. Hu, Excellent photocatalytic degradation of tetracycline over black anatase-TiO_2 under visible light, *Chem. Eng. J.*, 2021, **406**, 126747.

3 S. Wu, H. Hu, Y. Lin, J. Zhang, Y.H. Hu, Visible light photocatalytic degradation of tetracycline over TiO_2, *Chem. Eng. J.*, 2020, **382**, 122842.

4 P. Wang, P.S. Yap, T.T. Lim, C–N–S tridoped TiO_2 for photocatalytic degradation of tetracycline under visible-light irradiation, *Appl. Catal. A-Gen.*, 2011, **399**, 252–261.

5 D. Ma, W. Liu, Q. Chen, Z. Jin, Y. Zhang, J. Huang, T. Luo, Titanium-oxo-clusters precursors for preparation of In_2S_3/TiO_2 heterostructure and its photocatalytic degradation of tetracycline in water, *J. Solid State Chem.*, 2021, **293**, 121791.

6 X. He, L. Wang, C. Yi, G. Wu, Preparation of MoS_2@MIL-53(Fe)and catalytic degradation of antibiotics under visible light irradiation, *Environ. Sci. Technol.*, 2020, **43**, 13–19.

7 M. Qiao, H. Liu, J. Lv, G. Xu, X. Zhang, X. Shu, Y. Wu, Enhanced visible-light photocatalytic remediation of tetracycline hydrochloride by nanostructured BiOI homojunctions, *Nano*, 2019, **14**, 1950112.